Decentralized Hamiltonian Control of Isolated AC Microgrids: Theory & Design

Mohamed Toub, Ghassane Aniba, Mohamed Maaroufi
Department of Electrical Engineering
Mohammadia School of Engineering
Mohammed V University of Rabat
Rabat, Morocco
mohamedtoub@research.emi.ac.ma,
{ghassane,maaroufi}@emi.ac.ma

Rush D. Robinet III
Department of Mechanical Engineering
Michigan Technological University
Michigan, United States
rdrobine@mtu.edu

***Abstract*—Microgrids technology is the cornerstone of smart grid, the electricity network of the future. Based on distributed generation, microgrids can contribute to increase the penetration rate of renewable energy resources and hence reduce costs and gas emissions. This paper presents a new design methodology, based on Hamiltonian Surface Shaping and Power Flow Control (HSSPFC), for a decentralized control of isolated microgrids (ImGs) with multiple distributed energy resources (DERs). The local controllers insure the stability of the overall ImG while regulating the voltage at the point of common coupling (PCC) of their respective DERs. Each controller is synthesized independently, using only local information on the corresponding DER, its dedicated load, and the corresponding line. This decentralized control procedure guarantees scalability and plug-and-play (PnP) operations of the ImG.**

***Index Terms*—Decentralized control, distributed power generation, microgrids, smart grids, voltage source converters.**

I. Introduction

The control strategies for microgrids have been extensively discussed and documented in the technical literature [1]. These strategies are hierarchically divided into three control levels: primary control, secondary control, and tertiary control [2]. The primary control has the fastest response, and is responsible for load sharing among distributed energy resources (DERs), voltage and frequency regulation, and plug-and-play (PnP) capability for new DERs. The secondary control restores the voltage and frequency, in a centralized manner, by compensating the deviation caused by the primary control. Tertiary control guarantees economical and optimal operations of the microgrid on the long term.

Different control methods have been adopted for the primary control level. Two main categories can be identified [3]: 1) The active load sharing method that requires high bandwidth communication for power measurements and coordination between geographically dispersed DERs. While it ensures accurate load sharing, this method requires expensive communication infrastructure, and can cause the collapse of the entire microgrid in case of communication failure (single point of failure). 2) The droop characteristic method which is a communication-free method that tries to emulate the droop characteristics of synchronous machines for the power balance of electronically-coupled microgrids.

The primary control of isolated and autonomous microgrids has been well investigated in the recent years. Reference [4] proposes multivariable servomechanism control for an autonomous single-DER microgrid. A digital multivariable design of a voltage controller for a single-DER microgrid is presented in [5]. The control strategies of both references perform proper regulation of voltage and are robust to load parameter changes. However, they did not investigate the interactions between DER units, since they focused on single-DER microgrids. Reference [6] introduces a generalized decentralized robust control strategy for autonomous operation of a multi-DER microgrid. A centralized power management system collects measurements from the DER units, calculates power and voltage set points, and communicates these appropriate set points to the decentralized servomechanism controllers. The main drawbacks of this strategy are: 1) The power management system relies on a low-bandwidth communication, that will jeopardize the entire system in case of interruption or failure. 2) The design of the controllers is based on the model of the overall microgrid, which makes the scalability of the system very difficult. Reference [7] presents a decentralized control design procedure for isolated microgrids (ImGs) with meshed topology. The proposed design procedure enables PnP operations and maintains the stability and the performance of the ImG. Still, this design procedure is not fully decentralized as it requires, in addition to local information, the knowledge of two global scalar quantities.

This paper presents a decentralized control design based on Hamiltonian Surface Shaping and Power Flow Control (HSSPFC) [8] that overcomes the interdependency and scalability issues when synthesizing the decentralized controllers. The objective is to demonstrate that the local

Financial support from the Research Institute for Solar Energy and New Energies (IRESEN) is gratefully acknowledged.

controllers 1) can be designed independently using only the model of the correspondent subsystem, 2) can regulate the voltage at the point of common coupling (PCC) of their respective DERs, 3) can stabilize the overall ImG.

The rest of this paper is organized as follows. In Section II, we describe the ImG and present the dynamical state-space models of the subsystems and the overall ImG. HSSPFC decentralized control design is presented in Section III. Section IV investigates the ability of the local controllers to stabilize the overall ImG. Section V concludes this paper.

II. ISOLATED MICROGRID MODEL

In this section, we present the ImG studied in this paper and derive the state-space models. We consider the ImG in Fig. 1 consisting of a typical radial distribution feeder with N subsystems. Each subsystem k ($k=1,...,N$) is composed of:

- A DER unit represented by a dc voltage source (e.g. generic renewable energy source), a voltage sourced converter (VSC), and a series (R_{f_k}, L_{f_k}) filter.
- A dedicated load modeled as a three-phase parallel RLC network.
- A line with nonzero impedance (R_{t_k}, L_{t_k}), connecting the *kth* and the (k+1)*th* subsystems in a loop fashion (i.e. the last *Nth* subsystem is connected to the first subsystem).

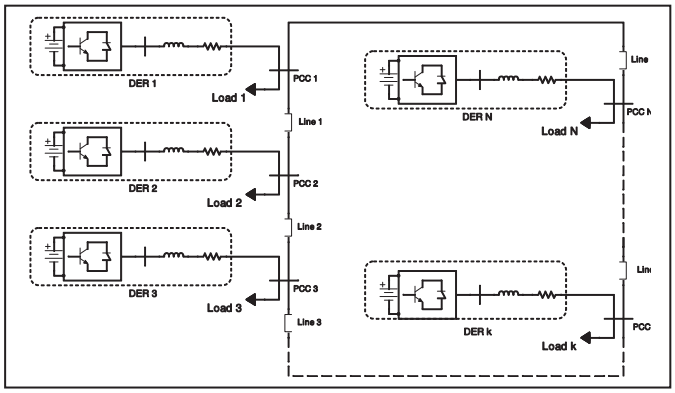

Figure 1. Schematic diagram of the isolated microgrid

The single-line diagram of the *kth* subsystem, shown in Fig. 2, is used to derive its state-space equations in the *abc*-frame for $k=1,...,N$:

$$\begin{cases} C_k \dfrac{dV_{k,abc}}{dt} = -\dfrac{V_{k,abc}}{R_k} + I_{k,abc} - I_{L_k,abc} - I_{t_k,abc} + I_{t_{(k-1)},abc} \\ L_{f_k} \dfrac{dI_{k,abc}}{dt} = -V_{k,abc} - R_{f_k} I_{k,abc} + V_{t_k,abc} \\ L_k \dfrac{dI_{L_k,abc}}{dt} = V_{k,abc} - R_{L_k} I_{L_k,abc} \\ L_{t_k} \dfrac{dI_{t_k,abc}}{dt} = V_{k,abc} - R_{tk} I_{t_k,abc} - V_{(k+1),abc} \end{cases} \quad (1)$$

Note that, for $k=1$, $I_{t_{(k-1)}} = I_{t_N}$ which corresponds to the line current of the *Nth* subsystem, and for $k=N$, $V_{(k+1)} = V_1$ which corresponds to the voltage at the PCC of the first subsystem.

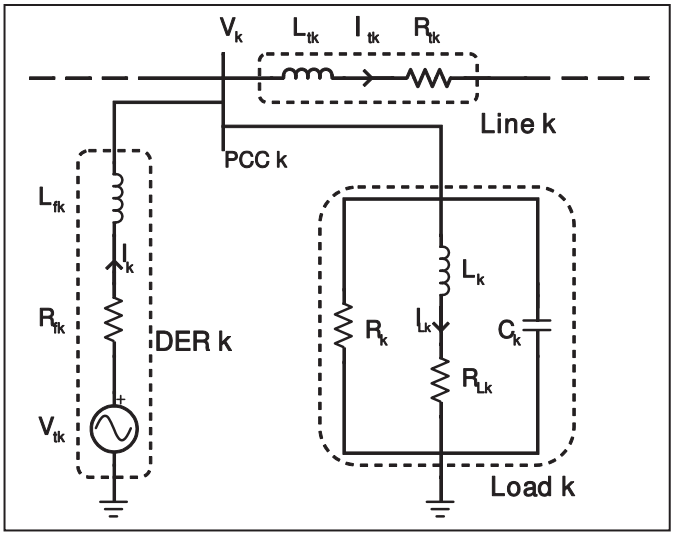

Figure 2. Single-line diagram of the *kth* subsystem

Each variable in (1) is a 3×1 vector composed of the three phase quantities. Assuming balanced three-phase subsystems, we apply the Park's transformation to (1) and derive the state-space model of the *kth* subsystem in a *dq*-frame rotating with speed ω_0, giving

$$\begin{cases} C_k \dfrac{dV_{k,d}}{dt} = \dfrac{-V_{k,d}}{R_k} + \omega_0 C_k V_{k,q} + I_{k,d} - I_{L_k,d} - I_{t_k,d} + I_{t_{(k-1)},d} \\ C_k \dfrac{dV_{k,q}}{dt} = -\omega_0 C_k V_{k,d} - \dfrac{V_{k,q}}{R_k} + I_{k,q} - I_{L_k,q} - I_{t_k,q} + I_{t_{(k-1)},q} \\ L_{f_k} \dfrac{dI_{k,d}}{dt} = -V_{k,d} - R_{f_k} I_{k,d} + \omega_0 L_{f_k} I_{k,q} + V_{t_k,d} \\ L_{f_k} \dfrac{dI_{k,q}}{dt} = -V_{k,q} - \omega_0 L_{f_k} I_{k,d} - R_{f_k} I_{k,q} + V_{t_k,q} \\ L_k \dfrac{dI_{L_k,d}}{dt} = V_{k,d} - R_{L_k} I_{L_k,d} + \omega_0 L_k I_{L_k,q} \\ L_k \dfrac{dI_{L_k,q}}{dt} = V_{k,q} - \omega_0 L_k I_{L_k,d} - R_{L_k} I_{L_k,q} \\ L_{t_k} \dfrac{dI_{t_k,d}}{dt} = V_{k,d} - R_{t_k} I_{t_k,d} + \omega_0 L_{t_k} I_{t_k,q} - V_{(k+1),d} \\ L_{t_k} \dfrac{dI_{t_k,q}}{dt} = V_{k,q} - \omega_0 L_{t_k} I_{tk,d} - R_{t_k} I_{k,q} - V_{(k+1),q} \end{cases} \quad (2)$$

The subsystem equations (2) can be represented as a descriptor state space model with the following form:

$$\begin{cases} E_k \dot{x}_k(t) = A_{kk} x_k(t) + B_k u_k(t) + \xi_k(t) \\ y_k(t) = C_k x_k(t) \end{cases} \quad (3)$$

where $x_k = [V_{k,d}, V_{k,q}, I_{k,d}, I_{k,q}, I_{L_k,d}, I_{L_k,q}, I_{t_k,d}, I_{t_k,q}]^T$, $u_k = [V_{t_k,d}, V_{t_k,q}]^T$, $y_k = [V_{k,d}, V_{k,q}]^T$ are the state, the control input, and the controlled output of the *kth* subsystem, respectively. $\xi_k = A_{kk-1}x_{k-1} + A_{kk+1}x_{k+1}$ is the coupling interaction with both the *(k-1)th* and the *(k+1)th* subsystems. The matrices in (3) are

$$E_k = \begin{bmatrix} C_k & 0 & 0 & 0 & 0 & 0 & 0 & 0 \\ 0 & C_k & 0 & 0 & 0 & 0 & 0 & 0 \\ 0 & 0 & L_{f_k} & 0 & 0 & 0 & 0 & 0 \\ 0 & 0 & 0 & L_{f_k} & 0 & 0 & 0 & 0 \\ 0 & 0 & 0 & 0 & L_k & 0 & 0 & 0 \\ 0 & 0 & 0 & 0 & 0 & L_k & 0 & 0 \\ 0 & 0 & 0 & 0 & 0 & 0 & L_{t_k} & 0 \\ 0 & 0 & 0 & 0 & 0 & 0 & 0 & L_{t_k} \end{bmatrix}$$

$$A_{kk} = \begin{bmatrix} \frac{-1}{R_k} & \omega_0 C_k & 1 & 0 & -1 & 0 & -1 & 0 \\ -\omega_0 C_k & \frac{-1}{R_k} & 0 & 1 & 0 & -1 & 0 & -1 \\ -1 & 0 & -R_{f_k} & \omega_0 L_{f_k} & 0 & 0 & 0 & 0 \\ 0 & -1 & -\omega_0 L_{f_k} & -R_{f_k} & 0 & 0 & 0 & 0 \\ 1 & 0 & 0 & 0 & -R_{L_k} & \omega_0 L_k & 0 & 0 \\ 0 & 1 & 0 & 0 & -\omega_0 L_k & -R_{L_k} & 0 & 0 \\ 1 & 0 & 0 & 0 & 0 & 0 & -R_{t_k} & \omega_0 L_{t_k} \\ 0 & 1 & 0 & 0 & 0 & 0 & -\omega_0 L_{t_k} & -R_{t_k} \end{bmatrix}$$

$$A_{kk+1} = \begin{bmatrix} 0 & 0 & 0 & 0 & 0 & 0 & 0 & 0 \\ 0 & 0 & 0 & 0 & 0 & 0 & 0 & 0 \\ 0 & 0 & 0 & 0 & 0 & 0 & 0 & 0 \\ 0 & 0 & 0 & 0 & 0 & 0 & 0 & 0 \\ 0 & 0 & 0 & 0 & 0 & 0 & 0 & 0 \\ 0 & 0 & 0 & 0 & 0 & 0 & 0 & 0 \\ -1 & 0 & 0 & 0 & 0 & 0 & 0 & 0 \\ 0 & -1 & 0 & 0 & 0 & 0 & 0 & 0 \end{bmatrix} = -A_{kk-1}^T$$

$$B_k^T = \begin{bmatrix} 0 & 0 & 1 & 0 & 0 & 0 & 0 & 0 \\ 0 & 0 & 0 & 1 & 0 & 0 & 0 & 0 \end{bmatrix}$$

$$C_k = \begin{bmatrix} 1 & 0 & 0 & 0 & 0 & 0 & 0 & 0 \\ 0 & 1 & 0 & 0 & 0 & 0 & 0 & 0 \end{bmatrix}$$

Next, we derive the state-space model of the overall system. It is worth mentioning that the *N* subsystems are disjoint [9]. In other words, the states of the subsystems are not overlapping; a state space variable cannot be found in two different space vectors. Hence, the descriptor state-space model of the overall ImG is

$$\begin{cases} E\dot{x}(t) = Ax(t) + Bu(t) \\ y(t) = Cx(t) \end{cases} \tag{4}$$

where $x = (x_1, \ldots, x_N) \in \mathbb{R}^{8N}$, $u = (u_1, \ldots, u_N) \in \mathbb{R}^{2N}$ and $y = (y_1, \ldots, y_N) \in \mathbb{R}^{2N}$. The matrices in (4) are

$$E = \begin{bmatrix} E_1 & 0 & \cdots & 0 \\ 0 & E_2 & \cdots & 0 \\ \vdots & \vdots & \ddots & \vdots \\ 0 & 0 & \cdots & E_N \end{bmatrix}$$

$$A = \begin{bmatrix} A_{11} & A_{12} & 0 & \cdots & 0 & A_{1N} \\ A_{21} & \ddots & \ddots & 0 & \cdots & 0 \\ 0 & \ddots & \ddots & \ddots & \ddots & \vdots \\ \vdots & \ddots & \ddots & \ddots & \ddots & 0 \\ 0 & \cdots & 0 & \ddots & \ddots & A_{N-1N} \\ A_{N1} & 0 & \cdots & 0 & A_{NN-1} & A_{NN} \end{bmatrix}$$

$$B = \begin{bmatrix} B_1 & 0 & \cdots & 0 \\ 0 & B_2 & \cdots & 0 \\ \vdots & \vdots & \ddots & \vdots \\ 0 & 0 & \cdots & B_N \end{bmatrix} \quad C = \begin{bmatrix} C_1 & 0 & \cdots & 0 \\ 0 & C_2 & \cdots & 0 \\ \vdots & \vdots & \ddots & \vdots \\ 0 & 0 & \cdots & C_N \end{bmatrix}$$

III. DECENTRALIZED HSSPFC DESIGN

In this section, we present a decentralized control design procedure based on HSSPFC. The local controllers will be designed in a decentralized fashion based on the nominal model of the corresponding subsystem only, without requiring any information about the other subsystems.

We consider the nominal model of the *kth* subsystem without the coupling term ξ_k given by

$$\begin{cases} E_k \dot{x}_k(t) = (\bar{A}_{kk} + \tilde{A}_{kk})x_k(t) + B_k u_k(t) \\ y_k(t) = C_k x_k(t) \end{cases} \tag{5}$$

where A_{kk} is the sum of a diagonal matrix, $\bar{A}_{kk}$ and a skew-symmetric matrix, $\tilde{A}_{kk}$. Based on HSSPFC, we design a proportional-integral (PI) controller such that the nominal closed-loop subsystem is asymptotically stable. First, we define an error state for the nominal model (5)

$$\tilde{x}_k = x_{k,ref} - x_k \tag{6}$$

where $x_{k,ref}$ is the reference state. The values of the reference state can be set by the system designer, the droop calculation, or a power management system. Given the reference state $x_{k,ref}$, the reference control input, $u_{k,ref}$ is calculated from the following expression:

$$E_k \dot{x}_{k,ref}(t) = \left(\bar{A}_{kk} + \tilde{A}_{kk}\right) x_{k,ref}(t) + B_k u_{k,ref}(t) \quad (7)$$

From (5) and (7), the dynamics of the error state are given by

$$E_k \dot{\tilde{x}}_k(t) = \left(\bar{A}_{kk} + \tilde{A}_{kk}\right) \tilde{x}_k(t) + B_k \Delta u_k(t) \quad (8)$$

where $\Delta u_k = u_{k,ref} - u_k$.

Now, we choose the PI controller as

$$\Delta u_k = -K_{P_k} \tilde{x}_k - K_{I_k} \int_0^t \tilde{x}_k d\tau \quad (9)$$

where K_{P_k} and K_{I_k} are positive definite gain matrices. We replace Δu_k in (8) with the right-half side of (9)

$$E_k \dot{\tilde{x}}_k(t) = \left(\bar{A}_{kk} + \tilde{A}_{kk} - B_k K_{P_k}\right) \tilde{x}_k - B_k K_{I_k} \int_0^t \tilde{x}_k d\tau. \quad (10)$$

Hence, the model of the *kth* closed-loop subsystem is

$$\begin{bmatrix} E_k & 0 \\ 0 & B_k K_{I_k} \end{bmatrix} \begin{bmatrix} \dot{\tilde{x}}_k \\ \dot{\tilde{v}}_k \end{bmatrix} = \begin{bmatrix} \bar{A}_{kk} + \tilde{A}_{kk} - B_k K_{P_k} & -B_k K_{I_k} \\ B_k K_{I_k} & 0 \end{bmatrix} \begin{bmatrix} \tilde{x}_k \\ \tilde{v}_k \end{bmatrix} \quad (11)$$

where $\tilde{v}_k = \int_0^t \tilde{x}_k d\tau$, and $\hat{x}_k = (\tilde{x}_k, \tilde{v}_k)$ is the state of the closed-loop subsystem.

Next, we define the Hamiltonian of the *kth* closed-loop subsystem as

$$\begin{aligned} H_k(\hat{x}_k) &= \frac{1}{2} \hat{x}_k^T \begin{bmatrix} E_k & 0 \\ 0 & B_k K_{I_k} \end{bmatrix} \hat{x}_k \\ &= \frac{1}{2} \begin{bmatrix} \tilde{x}_k \\ \tilde{v}_k \end{bmatrix}^T \begin{bmatrix} E_k & 0 \\ 0 & B_k K_{I_k} \end{bmatrix} \begin{bmatrix} \tilde{x}_k \\ \tilde{v}_k \end{bmatrix} \\ &= \frac{1}{2} \tilde{x}_k{}^T E_k \tilde{x}_k + \frac{1}{2} \left(\int_0^t \tilde{x}_k^T d\tau\right) B_k K_{I_k} \left(\int_0^t \tilde{x}_k d\tau\right). \end{aligned} \quad (12)$$

E_k is positive definite, and by choosing K_{I_k} such as $B_k K_{I_k}$ is also positive definite, we will guarantee the static stability condition: $H_k > 0$ [8] which is a necessary condition for stability. The time derivative of the Hamiltonian is

$$\begin{aligned} \dot{H}_k(\hat{x}_k) &= \tilde{x}_k^T E_k \dot{\tilde{x}}_k + \tilde{x}_k^T B_k K_{I_k} \int_0^t \tilde{x}_k d\tau \\ &= \tilde{x}_k^T [E_k \dot{x}_{k,ref} - E_k \dot{x}_k] + \tilde{x}_k^T B_k K_{I_k} \int_0^t \tilde{x}_k d\tau \\ &= \tilde{x}_k^T \Big[\left(\bar{A}_{kk} + \tilde{A}_{kk}\right) x_{k,ref} + B_k u_{k,ref} \\ &\quad - \left(\bar{A}_{kk} + \tilde{A}_{kk}\right) x_k - B_k u_k \Big] + \tilde{x}_k^T B_k K_{I_k} \int_0^t \tilde{x}_k d\tau \\ &= \tilde{x}_k^T \left(\bar{A}_{kk} + \tilde{A}_{kk}\right) \tilde{x}_k + \tilde{x}_k^T B_k (u_{k,ref} - u_k) \\ &\quad + \tilde{x}_k^T B_k K_{I_k} \int_0^t \tilde{x}_k d\tau \\ &= \tilde{x}_k^T \left(\bar{A}_{kk} + \tilde{A}_{kk}\right) \tilde{x}_k + \tilde{x}_k^T B_k \Delta u_k + \tilde{x}_k^T B_k K_{I_k} \int_0^t \tilde{x}_k d\tau \end{aligned} \quad (13)$$

since $\tilde{A}_{kk}$ is a skew-symmetric matrix, $\tilde{x}_k^T \tilde{A}_{kk} \tilde{x}_k = 0$.

$$\begin{aligned} \dot{H}_k(\hat{x}_k) &= \tilde{x}_k^T \bar{A}_{kk} \tilde{x}_k - \tilde{x}_k^T B_k K_{P_k} \tilde{x}_k \\ &\quad - \tilde{x}_k^T B_k K_{I_k} \int_0^t \tilde{x}_k d\tau + \tilde{x}_k^T B_k K_{I_k} \int_0^t \tilde{x}_k d\tau \\ &= -\tilde{x}_k^T \left(B_k K_{P_k} - \bar{A}_{kk}\right) \tilde{x}_k \le 0, \ \forall \hat{x}_k \ne 0 \end{aligned} \quad (14)$$

Equations (12) and (14) guide the choice of the PI controller gains. Furthermore, since the Hamiltonian derivative is negative semi definite, the subsystem is not necessary asymptotically stable. In order to prove asymptotic stability, the higher order derivatives of the Hamiltonian (the Lyapunov function candidate) are investigated [10].

Theorem. [10]

Assume there exists a Lyapunov function V(x) of the dynamical system $\dot{x} = f(x)$. *Let* Ω *be a non-empty set of state vectors such that*

$$x \in \Omega \Rightarrow \dot{V}(x) = 0.$$

If the first k-1 derivatives of V(x), evaluated on the set Ω, *are zero*

$$\frac{d^i V(x)}{dt^i} = 0 \qquad \forall x \in \Omega \qquad i = 1, 2, ..., \mathrm{k}-1$$

and the kth derivative is negative definite on the set Ω

$$\frac{d^i V(x)}{dt^i} < 0 \qquad \forall x \in \Omega$$

then the system x(t) is asymptotically stable, if k is an odd number.

We apply this **Theorem.** to our closed-loop subsystem, and we consider the Hamiltonian from (12) as a Lyapunov function candidate. The set of state vectors Ω_k where

$$\hat{x}_k \in \Omega_k \Rightarrow \dot{H}_k(\hat{x}_k) = 0$$

is

$$\Omega_k = \left\{ \hat{x}_k = (\tilde{x}_k, \int_0^t \tilde{x}_k) \,\middle|\, \tilde{x}_k = 0 \right\}.$$

For the first order time derivative of the Hamiltonian (12), we have

$$\dot{H}_k = -\tilde{x}_k^T \left(B_k K_{P_k} - \bar{A}_{kk}\right) \tilde{x}_k = 0 \quad \text{for} \quad \tilde{x}_k = 0 \quad (15)$$

then

$$\dot{H}_k(\hat{x}_k) = 0 \quad \forall \hat{x}_k \in \Omega_k. \quad (16)$$

For the second order time derivative of the Hamiltonian, we find

$$\begin{aligned}\ddot{H}_k &= -2\tilde{x}_k^T\left(B_kK_{P_k}-\bar{A}_{kk}\right)\dot{\tilde{x}}_k\\ &= -2\tilde{x}_k^T\left(B_kK_{P_k}-\bar{A}_{kk}\right)E_k^{-1}E_k\dot{\tilde{x}}_k\\ &= -2\tilde{x}_k^T\left(B_kK_{P_k}-\bar{A}_{kk}\right)E_k^{-1}\Big[\left(A_{kk}-B_kK_{P_k}\right)\tilde{x}_k\\ &\quad -B_kK_{I_k}\int_0^t\tilde{x}_k d\tau\Big]\\ &= 0 \quad \text{for} \quad \tilde{x}_k=0\end{aligned} \tag{17}$$

then

$$\ddot{H}_k(\hat{x}_k)=0 \quad \forall\hat{x}_k\in\Omega_k. \tag{18}$$

The third order time derivative of the Hamiltonian is

$$\begin{aligned}\dddot{H}_k &= -2\dot{\tilde{x}}_k^T(B_kK_{P_k}-\bar{A}_{kk})E_k^{-1}\Big[(A_{kk}-B_kK_{P_k})\tilde{x}_k\\ &\quad -B_kK_{I_k}\int_0^t\tilde{x}_k d\tau\Big]-2\tilde{x}_k^T(B_kK_{P_k}-\bar{A}_{kk})E_k^{-1}\\ &\quad \Big[(A_{kk}-B_kK_{P_k})\dot{\tilde{x}}_k-B_kK_{I_k}\tilde{x}_k\Big]\\ &= -2\Big[E_k^{-1}\Big[(A_{kk}-B_kK_{P_k})\tilde{x}_k-B_kK_{I_k}\int_0^t\tilde{x}_k d\tau\Big]\Big]^T\\ &\quad (B_kK_{P_k}-\bar{A}_{kk})E_k^{-1}\Big[(A_{kk}-B_kK_{P_k})\tilde{x}_k\\ &\quad -B_kK_{I_k}\int_0^t\tilde{x}_k d\tau\Big]-2\tilde{x}_k^T(B_kK_{P_k}-\bar{A}_{kk})E_k^{-1}\\ &\quad \Big[(A_{kk}-B_kK_{P_k})E_k^{-1}[(A_{kk}-B_kK_{P_k})\tilde{x}_k\\ &\quad -B_kK_{I_k}\int_0^t\tilde{x}_k d\tau]-B_kK_{I_k}\tilde{x}_k\Big]\end{aligned} \tag{19}$$

for $\tilde{x}_k=0$ we have

$$\begin{aligned}\dddot{H}_k(\hat{x}_k) &= -2[E_k^{-1}B_kK_{I_k}\int_0^t\tilde{x}_k d\tau]^T(B_kK_{P_k}\\ &\quad -\bar{A}_{kk})\Big[E_k^{-1}B_kK_{I_k}\int_0^t\tilde{x}_k d\tau\Big]\end{aligned} \tag{20}$$

then

$$\dddot{H}_k(\hat{x}_k)<0 \quad \forall\hat{x}_k\in\Omega_k. \tag{21}$$

Since the first non-zero higher order derivative of H_k is of odd order and is negative definite on Ω_k, the *kth* closed-loop subsystem is asymptotically stable.

IV. Decentralized Control of the ImG

After designing controllers in a decentralized manner , we investigate, in this section, the ability of this decentralized controllers to stabilize the overall ImG.

We define an error state for the overall ImG system (4)

$$\tilde{x}=x_{ref}-x \tag{22}$$

where $\tilde{x}=(\tilde{x}_1,\ldots,\tilde{x}_N)$ and $x_{ref}=(x_{ref,1},\ldots,x_{ref,N})$.

Now, we define the Hamiltonian of the overall closed-loop system as

$$H=\frac{1}{2}\tilde{x}^TE\tilde{x}+\frac{1}{2}\left(\int_0^t\tilde{x}_k^T d\tau\right)BK_I\left(\int_0^t\tilde{x}_k d\tau\right) \tag{23}$$

where $K_I=diag(K_{I_1},\ldots,K_{I_N})$. E and BK_I are positive definite. Thus, the Hamiltonian H is also positive definite, and the overall ImG is statically stable. The time derivative of the Hamiltonian is

$$\begin{aligned}\dot{H}(\hat{x}) &= \tilde{x}^TE\dot{\tilde{x}}+\tilde{x}^TBK_I\int_0^t\tilde{x}d\tau\\ &= \tilde{x}^T(E\dot{x}_{ref}-E\dot{x})+\tilde{x}^TBK_I\int_0^t\tilde{x}d\tau\\ &= \tilde{x}^T(Ax_{ref}+Bu_{ref}-Ax-Bu)\\ &\quad +\tilde{x}^TBK_I\int_0^t\tilde{x}d\tau\\ &= \tilde{x}^TA\tilde{x}+\tilde{x}^TB(u_{k,ref}-u)+\tilde{x}^TBK_I\int_0^t\tilde{x}d\tau\\ &= \tilde{x}^TA\tilde{x}+\tilde{x}^TB\Delta u+\tilde{x}^TBK_I\int_0^t\tilde{x}d\tau\end{aligned} \tag{24}$$

where $\Delta u=(\Delta u_1,\ldots,\Delta u_N)$, and

$$\Delta u=-K_P\tilde{x}-K_I\int_0^t\tilde{x}d\tau \tag{25}$$

with $K_P=diag(K_{P_1},\ldots,K_{P_N})$. Note that for all $k\in\{1,\ldots,N\}$, $A_{kk+1}=-A_{k+1k}^T$ and $A_{kk}=\tilde{A}_{kk}+\bar{A}_{kk}$. Which proves that A can also be written as the sum of a diagonal matrix, $\bar{A}=diag(\bar{A}_{kk})$ and a skew-symmetric matrix, $\tilde{A}=A-\bar{A}$, then $\tilde{x}^T\tilde{A}\tilde{x}=0$ and

$$\begin{aligned}\dot{H}(\hat{x}) &= \tilde{x}^T\bar{A}\tilde{x}-\tilde{x}^TBK_P\tilde{x}\\ &\quad -\tilde{x}^TBK_I\int_0^t\tilde{x}d\tau+\tilde{x}^TBK_I\int_0^t\tilde{x}d\tau\\ &= -\tilde{x}^T(BK_P-\bar{A})\tilde{x}\\ &= \sum_{k=1}^N\Big[-\tilde{x}_k^T\left(B_kK_{P_k}-\bar{A}_{kk}\right)\tilde{x}\Big]\\ &= \sum_{k=1}^N\dot{H}_k\le 0, \ \forall\hat{x}\neq 0.\end{aligned} \tag{26}$$

For asymptotic stability, the time derivative of the Hamiltonian $\dot{H}$ is required to be negative definite. Thus, we should investigate the higher order derivatives of the Hamiltonian in order to prove asymptotic stability.

We calculate the second order derivative of the Hamiltonian:

From (26), the set Ω where $\dot{H}=0$ is $\Omega=\Omega_1\times\ldots\times\Omega_N$. We calculate the second order derivative of the Hamiltonian:

$$\begin{aligned}\ddot{H} &= \frac{d\dot{H}}{dt}\\ &= \sum_{k=1}^N\ddot{H}_k\\ &= 0 \quad \forall\hat{x}\in\Omega.\end{aligned} \tag{27}$$

The third order derivative of the Hamiltonian of the overall closed-loop ImG is

$$\ddot{H} = \sum_{k=1}^{N} \ddot{H}_k < 0 \quad \forall \hat{x} \in \Omega. \tag{28}$$

Therefore, the overall closed-loop system is asymptotically stable. This result proves the ability of the decentralized controllers to stabilize the overall ImG.

V. Results and Discussions

In this paper, a new method to design controllers for a decentralized control of ImGs with multiple DERs was presented. We should note that:

1) The HSSPFC decentralized controller can guarantee stability and increase performance of the overall system. Indeed, the eigenvalues of the overall closed-loop system, shown in Fig. 3, are more distant from the imaginary axis than those of the overall open-loop system, which means that the time response of the overall system is improved.

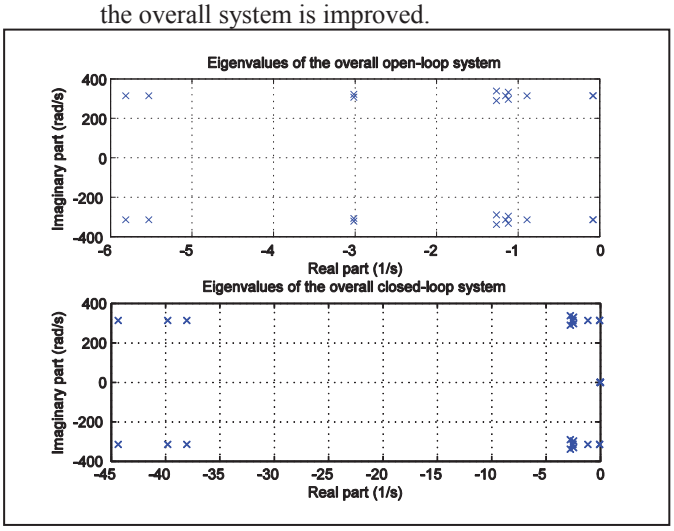

Figure 3. Eigenvalues of the overall open-loop and closed-loop systems

2) By designing decentralized controllers that stabilize the overall system; using only local information on the corresponding DER, its dedicated load, and the corresponding line; we have theoretically showed that this method guarantees scalability and offers PnP operations.
3) In future work, the proposed method will be used to perform modeling and simulation of our new testbed, at the Mohammadia School for Engineering in Rabat, that requires scalable controllers with the PnP feature.

VI. Conclusion

The goal of this paper was to demonstrate that the proposed decentralized control design approach guarantees stability and performance, and facilitates the scalability and the PnP operations of new DERs in the ImG. The mathematical equations of the ImG were developed, and the state space models of the subsystems were derived. Hamiltonian Surface Shaping and Power Flow Control was used to design decentralized local controllers that stabilize the overall ImG, relying only on local information.

Acknowledgment

The authors gratefully acknowledge the contributions of Professor Wayne Weaver and Ms. Hasnae Bilil to this paper.

References

[1] D. E. Olivares et al., "Trends in microgrid control," *IEEE Trans. Smart Grid*, vol. 5, no. 4, pp. 1905–1919, Jul. 2014.

[2] A. Bidram and A. Davoudi, "Hierarchical structure of microgrids control system," *IEEE Trans. Smart Grid*, vol. 3, no. 4, pp. 1963–1976, Dec. 2012.

[3] N. Yang, D. Paire, F. Gao, and A. Miraoui, "Power management strategies for microgrid-A short review," in *Industry Applications Society Annual Meeting, 2013 IEEE*, 2013, pp. 1–9.

[4] H. Karimi, E. J. Davison, and R. Iravani, "Multivariable servomechanism controller for autonomous operation of a distributed generation unit: design and performance evaluation," *IEEE Trans. Power Syst.*, vol. 25, no. 2, pp. 853–865, May 2010.

[5] B. Bahrani, M. Saeedifard, A. Karimi, and A. Rufer, "A multivariable design methodology for voltage control of a single-DG-unit microgrid," *IEEE Trans. Ind. Inform.*, vol. 9, no. 2, pp. 589–599, May 2013.

[6] A. H. Etemadi, E. J. Davison, and R. Iravani, "A generalized decentralized robust control of islanded microgrids," *IEEE Trans. Power Syst.*, vol. 29, no. 6, pp. 3102–3113, Nov. 2014.

[7] S. Riverso, F. Sarzo, and G. Ferrari-Trecate, "Plug-and-Play voltage and frequency control of islanded microgrids with meshed topology," *IEEE Trans. Smart Grid*, vol. 6, no. 3, pp. 1176–1184, May 2015.

[8] R. D. Robinett, D. G. Wilson, and SpringerLink (Online service), *Nonlinear power flow control design utilizing exergy, entropy, static and dynamic stability, and Lyapunov analysis*. London; New York: Springer, 2011.

[9] J. Lunze, *Feedback control of large scale systems*. New York: Prentice-Hall, 1992.

[10] W. W. Weaver, R. D. Robinett, G. G. Parker, and D. G. Wilson, "Distributed control and energy storage requirements of networked dc microgrids," *Control Eng. Pract.*, vol. 44, pp. 10–19, Nov. 2015.